

## **HEAT TRANSFER MODELLING OF CANDU PRESSURE TUBE UNDER LOCALIZED HIGH TEMPERATURE CONDITION**

F. TALEBI, J.C. LUXAT

McMaster University, Engineering Physics Department, Hamilton, Ontario, Canada L8S 4L7  
e-mail: farshat@mcmaster.ca, luxatj@mcmaster.ca

### **ABSTRACT**

The main objective of this research is to develop thermal models in order to evaluate mechanical deformation of the potential contacts between fuel elements and pressure tube in the CANDU reactor. The consequence of concern is potential creep strain failure of a pressure tube and calandria tube challenging fuel channel integrity. The initial focus will be on the case where a fuel rod contacts the pressure tube at full power with high cooling flow. Such an event could occur if a fuel element was to become detached from a bundle. The heat conduction from fuel sheath to the inner surface of the pressure tube with appropriate convective and radiation boundary conditions has been simulated. The contact boundary could be a single spot or a small arc between the fuel sheath and pressure tube. The vapor pockets are considered in the areas beside the contact region where the convective cooling is drastically decreased. Subsequently, modelling has been extended to the contact of number of fuel elements where several fuel rods are postulated to contact the pressure tube under fully cooling conditions. It is observed that pressure tube creep strain will occur if sufficiently high temperature is reached.

### **1. INTRODUCTION**

The typical CANDU fuel assembly is a 37 rod cluster fuelled with natural uranium oxide and clad with zircaloy-4 (Figure 1(a)). The fuel assemblies are located inside a pressure tube made of zirconium with 2.5% niobium containing heavy water coolant. This pressure tube is separated by an annular gas-filled insulation gap from the zircaloy-2 calandria tube which is immersed in a heavy water moderator.

Normally the fuel elements (FEs) are not in direct contact with the pressure tube (PT) other than at the bearing pads of the outer elements at the bottom of the bundle. Should a severe bundle defect occur, it can be postulated that an element becomes detached from the bundle and sits in contact with the pressure tube. This highly unlikely condition is postulated to occur at full power and normal coolant flows and the resulting heat transfer is analyzed to determine the potential consequences of such an event. The contact boundary between the element and pressure tube is considered using the geometry depicted in Figure 1(b). The contact boundary could be either a single spot or a small arc depending on the bundle weight and location.

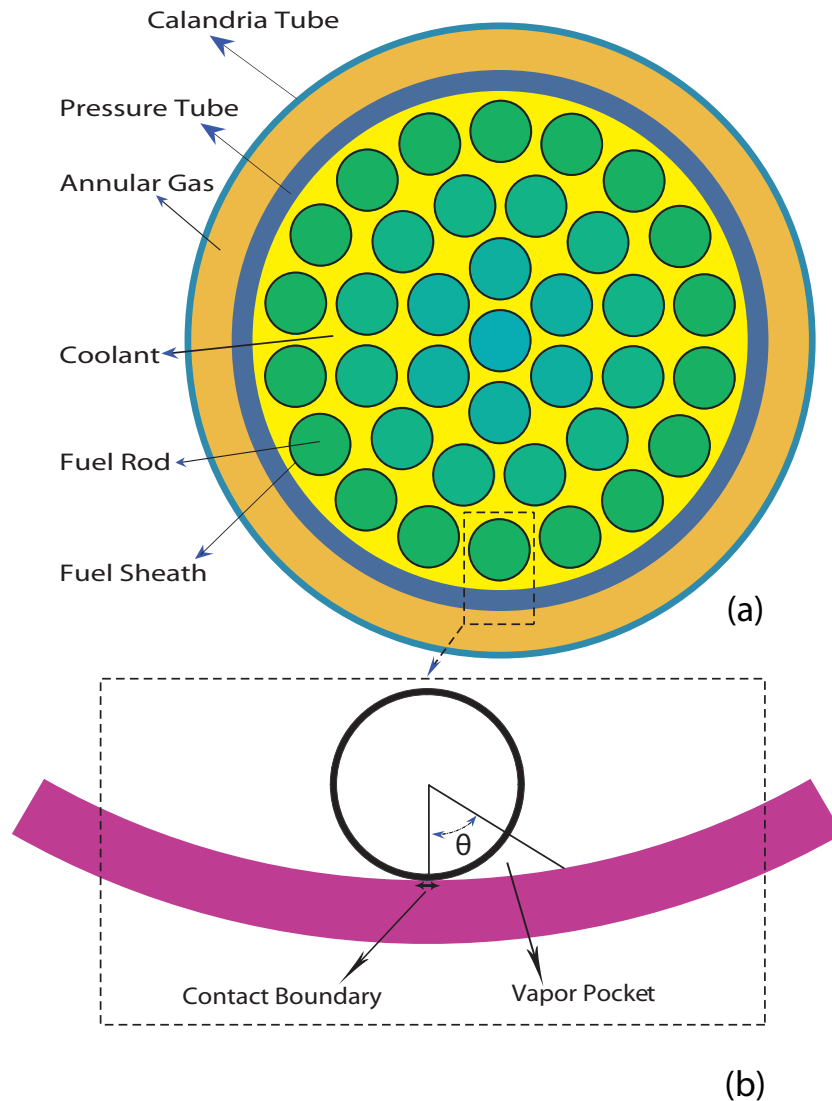


Figure 1. Standard CANDU-6 (a) and when FE/PT contact occurs (b)

As a consequence of localized degraded cooling in the region of contact the coolant could be vaporized on either side of the contact region, creating vapor pockets. These vapor pockets might be extended even more (increasing  $\theta$ ) depending on the heat flux of the fuel element and coolant conditions. During such reduction in convective cooling along with the extension of vapor pockets if sufficient heat is transferred to the pressure tube through conduction and radiation, then local deformation of the pressure tube may occur. In fact, zircaloy creep strain is significantly increased at temperatures greater than approximately 900 K due to  $\alpha$  to  $\beta$  phase change.<sup>[1,2]</sup>

A number of analytical and experimental studies have been performed and published. One of the earlier studies has been presented by McGee et al.,<sup>[3]</sup> where theoretical models were made and compared with the experimental analysis. The main goal was to evaluate overall thermal

resistance of a joint (consisting of a smooth right circular cylinder in contact with a smooth flat surface). A line contact model was considered to evaluate the thermal resistance of the solid to solid contact (i.e., cylinder to flat contact). For the thermal resistance of the gas-filled gaps on either side of the contact, three different models were constructed, i.e., the decoupled model (DCM), the half-space model (HSM) and the parallel flux-tube model (PFTM). These three models differ in the method used to calculate the temperature drop across the joint. Therefore, the total joint resistance was obtained using parallel summation of solid to solid contact with gas-gap thermal resistances. Experimental measurements of the overall thermal resistance were performed in vacuum and with a fluid and the effect of contact pressure was investigated for mechanical loads on specimens fabricated from Keewatin tool steel, stainless steel (type 304) and zircaloy-4. Finally, the authors compared the experimental data with the model predictions and large differences were observed between model and measurement except for a limited range of experimental parameters.

Another interesting study was performed by Reeves et al.<sup>[4]</sup> The authors presented analytical models which predict the transient thermal-mechanical behavior of a pressure tube following the contact of a hot fuel element under loss of coolant accident (LOCA) conditions. The code MINI-SMARTT was developed, based on finite difference techniques to solve the heat conduction equations with radiation and convection to the coolant and contact conduction between any specified number of fuel elements and pressure tube. A ring radiation model has been considered in order to simplify surface to surface radiation model for entire 37 fuel elements. This approach produced conservatively high radiation heat fluxes to the region of the pressure tube near the contact point. Using the code NUBALL, creep strain analysis associated with FE/PT contact was performed over a very broad range of calculations and a number of different cases. From the results of sensitivity analysis, the author concluded that the most sensitive parameters relevant to FE/PT contact were the contact conductance, transient time of the contact and contact width.

The MINI-SMARTT code was also used to investigate the effect of bearing pad (BP) to pressure tube (PT) contact and the code was validated using contact experimental results obtained at AECL-WRL.<sup>[5]</sup> Zircaloy oxidation at the fuel channel surfaces which drastically decreases the thermal conductivity of any zircaloy components was also considered.<sup>[6]</sup> They observed that the contact conductance of BP/PT contact was the most important parameter which did not remain constant during heating of the fuel bundle. It increased significantly until a threshold temperature was reached and then decreased, once local bulging allowed the pressure tube to deform away from the bearing pad. The authors concluded that contact conductances are small enough to ensure fuel channel integrity when single or multiple bearing pad contact occurs.

Muir et al.,<sup>[7]</sup> studied the case where the circumferential temperature gradient on the pressure tube is nonuniform resulting a nonuniform hoop stress and therefore a nonuniform pressure tube ballooning can occur which could result in pressure tube failure before occurrence of PT/CT contact. The pressure tube strain rate was calculated using the codes SMARTT and PTSTRAIN. Comparison presented with the code predictions against two different set of experiments which were performed with defected and non-defected pressure tubes at Stern Laboratories and at AECL. The authors explained that although slightly earlier failures were observed for non-defected tubes and slightly later failures predicted for defected tubes however, these could be

attributed to the approximations made in the model where the pressure tube was considered as a thin walled tube and remained circular during deformation.

During a postulated LOCA with failure of emergency core injection system (ECIS), if the pressure tube temperature increases sufficiently, the self-weight of the pressure tubes together with the weight of the fuel bundles could cause the pressure tube to sag into contact with the calandria tube. This might be accompanied simultaneously with pressure tube ballooning due to the internal pressure. Therefore, depending on the accident scenarios, other studies were performed either in experimental facilities or with analytical simulations using different computer codes in order to assess fuel channel integrity.<sup>[8-12]</sup> A very interesting study of complete coolant flow blockage of a single pressure tube in ACR-700 was performed by Gerardi et al.<sup>[13]</sup> The authors performed several thermal analysis in order to achieve a solid physical framework for the key phenomena of each stage of this accident using the finite element code COSMOSM. During the early stages of this accident the reactor remains at full power and full pressure, resulting in rapid coolant boil off and fuel overheating. Melting of the zircaloy components in the fuel bundle can occur, with relocation of some molten material to the bottom of the pressure tube, and therefore localized bulging of the pressure tube was predicted. According to Muir,<sup>[7]</sup> a 37% reduction in wall thickness of pressure tube from its initial value results in pressure tube and/or the calandria tube failure. They also concluded that a minimum molten zircaloy mass of about 100 g is required for failure of both the pressure tube and calandria tube.

None of the published papers considered any fuel element to pressure tube contact problem at full power and highly cooling conditions. The present research is focused on establishing the limits for maintaining fuel channel integrity for the situation in which fuel element to pressure tube contact occurs at full power and high coolant flow conditions. Therefore, we have attempted to simulate several analytical contact models which are the solutions to the steady state heat transfer equations along with appropriate boundary conditions as a primary analysis for mechanical deformation calculations. Several important key parameters affecting the contact modelling are introduced in order to perform sensitivity analysis.

## 2. DESCRIPTION OF THE MODELS

In a CANDU 37 element fuel bundle, four fuel rings containing respectively 1, 6, 12 and 18 fuel elements are considered (see Figure 1(a)). The pitch circle radius of each ring is 0.0 cm, 1.4884 cm, 2.8755 and 4.3305 cm, respectively. The fuel pellet radius is 0.6122 cm and the thickness of the sheath is 0.0418 cm. The inner radius of the pressure tube is 5.1689 cm and its thickness is 0.4343 cm. The gas gap between the pressure and calandria tubes is filled with carbon dioxide and the thickness of gap is 0.8446 cm.<sup>[14]</sup>

Fuel element to pressure tube contact is postulated to occur in a number of different ways. Two different cases are considered here, i.e., single fuel element-pressure tube contact (FE/PT) and a cluster of three fuel elements-pressure tube contact (3FE/PT) (see Figure 2). In the first case, the center of an outer fuel element is displaced radially by 0.1835 cm bringing it into contact with the inner surface of the pressure tube (Figure 2(a)). In the second case, three fuel elements are postulated to radially contact to the pressure tube, in the same way as the first

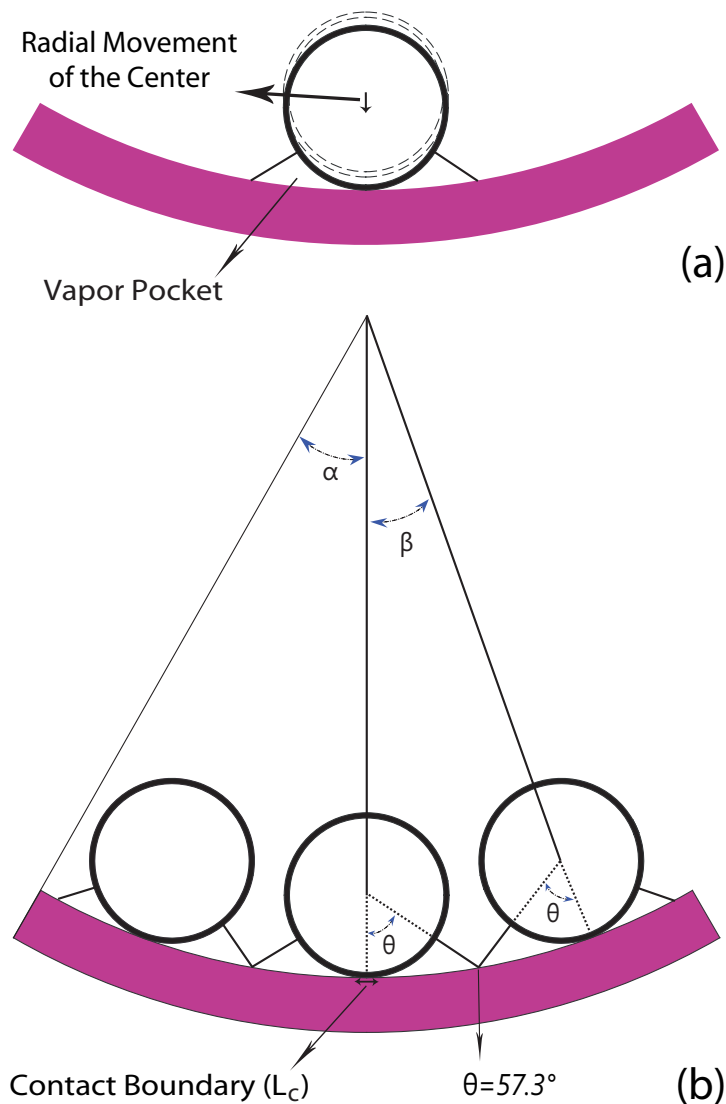


Figure 2. Single FE/PT contact (a) and 3FE/PT contact (b)

case (Figure 2(b)). Both cases are constructed with a pressure tube arc angle of  $2\alpha = 60^\circ$ . In the second case, the central locations of the fuel elements are maintained with in the same azimuthal step size of  $\beta = 20^\circ$ .

Coolant is vaporized in the both sides of the contact boundary due to the degraded cooling condition creating local vapor pockets. The extent of the vapor pockets depends on the heat flux of the fuel element and coolant conditions. In order to simulate such conditions, the vapor pocket dimensions, specified by  $\theta$ , is uniformly increased in both sides of each fuel element from  $15^\circ$  to  $57.3^\circ$  where are overlapped according to the Figure 2(b). However, the vapor in these pockets is considered to be stagnated due to the fact that vapor velocity is zero at the boundaries and therefore any motion or convection by vapor is not expected.<sup>[15]</sup> With regard to radiation heat transfer, a nonparticipating transparent medium is considered inside each vapor pocket that neither absorbs nor scatters the surface radiations and emits no radiation.<sup>[15]</sup>

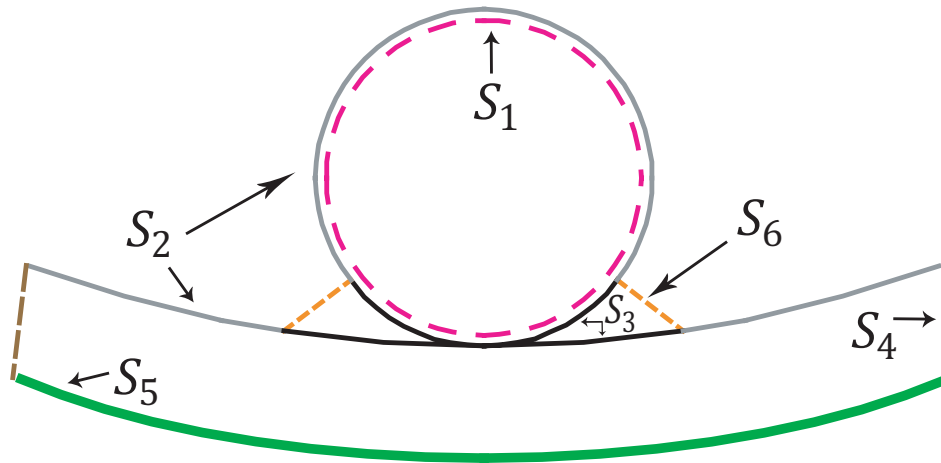


Figure 3. Single FE/PT contact boundaries

The steady state heat transfer equation (1) with appropriate convective and radiation boundary conditions (equation 2,3) are considered for the fuel sheath, pressure tube and transparent vapor pocket regions:

$$\vec{\nabla} \cdot k \vec{\nabla} T = 0 \quad : \Omega \quad (1)$$

$$\hat{n} \cdot \vec{q}'' = \vec{q}_0'' + h(T_{wall} - T_\infty) \quad : S_5 \quad (2)$$

$$(1 - \varepsilon)G = J - \varepsilon \sigma T^4 \implies q_{rad}'' = \varepsilon(G - \sigma T^4) \quad : S_3 \quad (3)$$

where  $k(T)$  denotes the thermal conductivity ( $W/mK$ ) as a function of temperature for each domain  $\Omega$ , i.e., zircaloy-4 fuel sheath, zirconium-2.5% niobium pressure tube and vapor regions which is obtained from the ZRPRO<sup>[16]</sup> and XSteam-Matlab joint function.<sup>[17]</sup> As is shown in Figure 3 only outward fuel element heat flux vector,  $\vec{q}_0'' = 1.5$  ( $MW/m^2$ ) is considered on the surface  $S_1$ , which is identical to that of  $\vec{q}_0'' = 60$  ( $kW/m$ ), a typical high linear rating power of outer elements in a CANDU fuel bundle. On the surface  $S_5$ , the heat transfer coefficient  $h=10$  ( $W/m^2K$ ) has been chosen without consideration of any extra heat sources.<sup>[13]</sup> The term  $\hat{n}$  is the normal unit vector at each boundary surface and the temperature of annulus gas gap has been taken as  $T_\infty = 180^\circ C$ .

When vapor pockets are created, radiative heat is transferred through these transparent regions and the inner surface of pressure tube gets hotter, hence, surface to surface radiation boundary conditions must be considered on the  $S_3$  surfaces. The zircaloy emissivity is considered as  $\varepsilon = 0.8$  and  $\sigma$  is Stefan-Boltzmann constant,  $G$  and  $J$  are the radiosity and irradiation, respectively. The  $S_2$  surface boundaries are considered to be at fully cooled condition with saturation temperature of coolant, i.e.,  $T = 310^\circ C$ .<sup>[18]</sup> On the  $S_6$  surface boundary where the coolant is reached to the vapor medium, we have assumed that the evaporation is at the equilibrium with condensation and therefore  $T = 310^\circ C$  is implemented. The symmetry boundary conditions

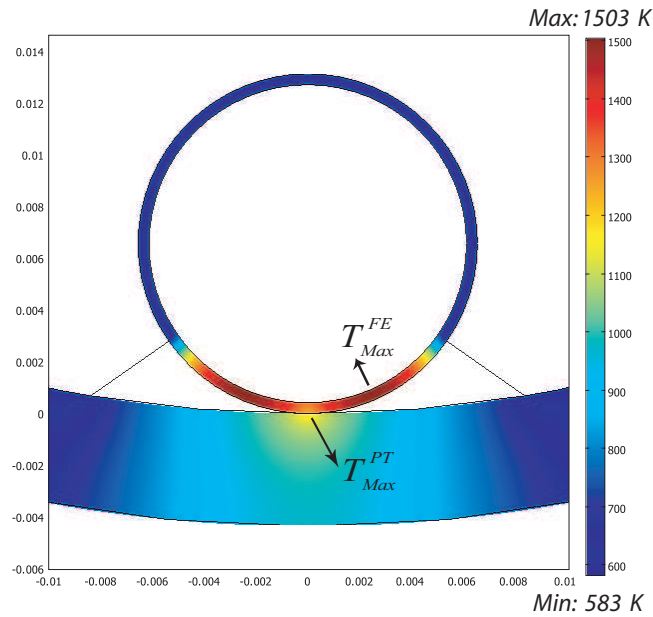


Figure 4. Temperature profile in FE/PT with spot contact and  $\theta = 55^\circ$  vapor pocket.

are also considered in both ends of the pressure tube  $S_4$ . The above equations and boundary conditions are simultaneously solved using the finite element method<sup>[19]</sup> in the COMSOL<sup>[20]</sup> software package.

All these calculations are strongly dependent on the consideration of the contact boundary between the fuel element and pressure tube.<sup>[4,21,22]</sup> In fact, knowing the pressure which acts on the contacting surfaces and the contact width ( $L_c$ ) are related to the bundle weight, direction, location and other contact circumstances in the fuel channel. However, the contact boundary could be either a single spot or a small arc. Therefore, two different set of simulations have been performed based on contact boundary, i.e., spot model simulation and arc model simulation.

## 2.1 SPOT MODEL SIMULATION

In this weightless model, a single spot with perfect contact condition is considered for either the FE/PT or 3FE/PT contact cases. In order to ensure spatial convergence, each domain and boundary must be subdivided into the fine regions. However, for those boundaries where surface to surface radiation condition ( $S_3$  in Figure 3) is considered even finer mesh element must be chosen. As a result, in the case of FE/PT contact, when  $\theta$  is changed from  $15^\circ$  to  $57.3^\circ$ , the number of mesh and degree of freedom<sup>[19]</sup> increased from 2230 and 11900 to 6640 and 19200, respectively. Similarly, in the case of 3FE/PT the number of mesh and degree of freedom risen accordingly, from 5130 and 26800 to 14800 and 46600.

Figure 4 shows the solution to the energy equation for the spot contact model (FE/PT case) where  $\theta = 55^\circ$ . The maximum temperature ( $T_{Max}^{FE} = 1503$  K) is obtained in the FE sheath domain while the pressure tube maximum temperature is found to be at spot contact boundary ( $T_{Max}^{PT} = 1207$  K). This is because of the fact that heat generated in the fuel pellet could properly

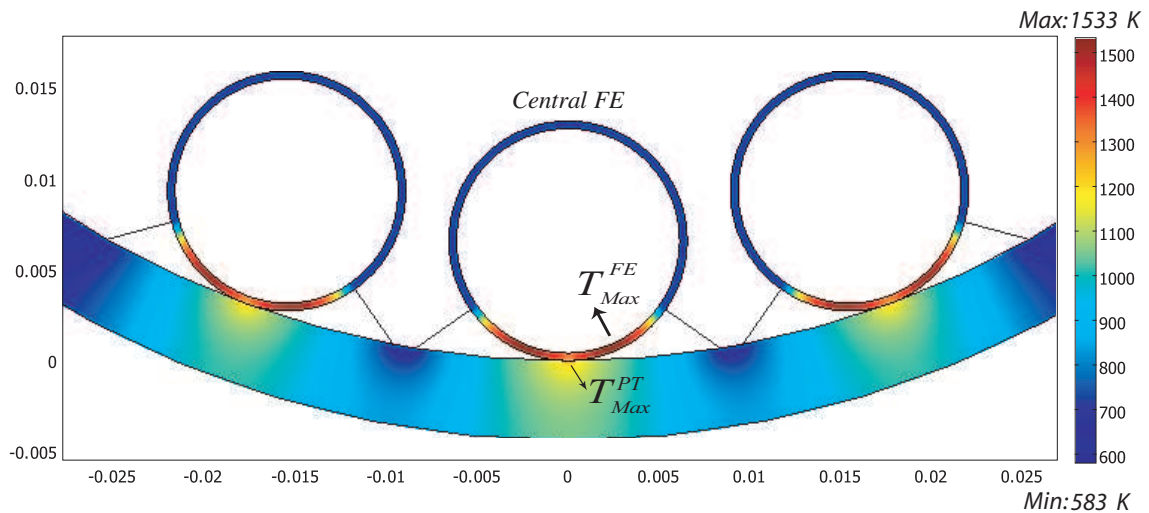


Figure 5. Temperature profile in 3FE/PT with spot contact and  $\theta = 55^\circ$  vapor pocket.

transfer into the coolant by convection but partially conducted to the PT through contact point and then transferred through PT thickness to the annulus gas gap. However, those hot regions are achieved due to the lack of proper cooling condition either by conduction, convection and radiation through the vapor pockets. The rest of domain is cooled and temperature remains practically unchanged at 583 K. Although, the maximum temperatures of the FE sheath and PT inner surface are increased when  $\theta$  increases, however, the behavior of temperature profile obtained for whole domain are pretty similar to that of  $\theta = 55^\circ$ .

Figure 5 shows the 3FE/PT contact case with constructed vapor pocket of  $\theta = 55^\circ$ . The maximum temperatures of the central FE sheath ( $T_{Max}^{FE}$ ) is increased by 30 K and by 17 K in the other fuel sheaths. Accordingly, the pressure tube maximum temperature ( $T_{Max}^{PT}$ ) is obtained as 1262 K at the central spot contact compare to that of 1237 K at the two other contacts. Obviously, from Figure 6 it can be seen that the maximum PT temperature increases by 55 K at the central contact compare to that of single FE/PT case. This is mainly due to the reduction of coolant in two parts of pressure tube where vapor pockets are being overlapped, as well as higher heat conduction from two other contact regions. According to Figure 6, the maximum pressure tube temperature even increases rapidly when vapor pocket dimension increases (corresponding to increasing  $\theta$ ) resulting in very little coolant contacting the pressure tube between the fuel elements. These results illustrate the sensitivity of the calculated pressure tube temperature to the assumed coolant boundary conditions.

## 2.2 ARC MODEL SIMULATION

Although, the weightless spot model has a very good estimation of temperature profiles in different contact cases, it can be reasonably assumed that a uniform reaction force develops over the contact area due to the fuel bundle weight. Based on Hertz theory<sup>[22]</sup> of elastic contact for cylindrical bodies, Reeves et al.,<sup>[4]</sup> obtained a width of contact as  $L_c = 0.015 \text{ mm}$  for a

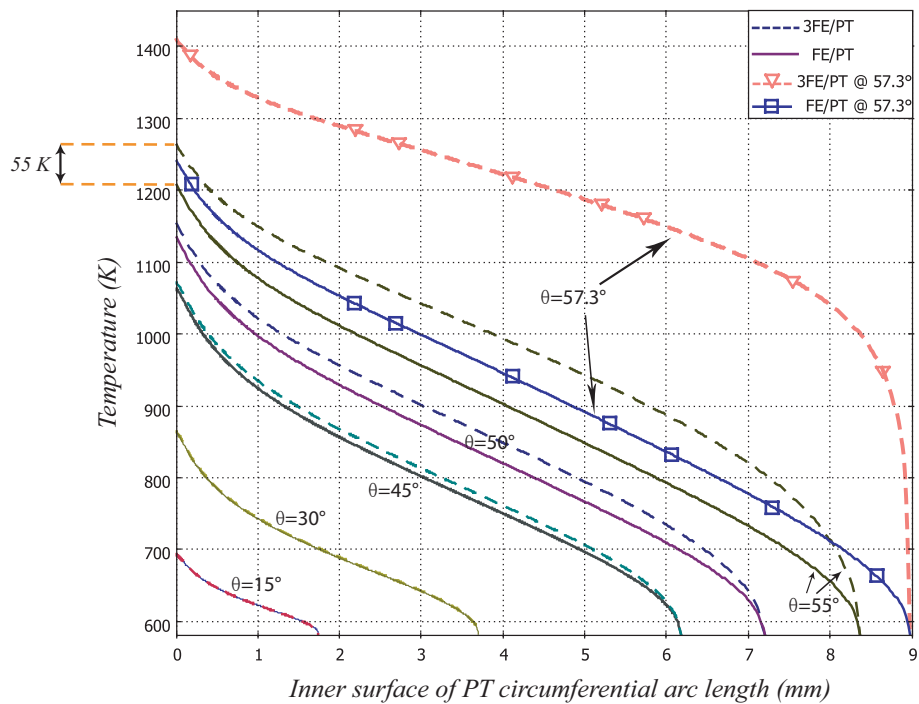


Figure 6. PT temperature profile in FE/PT and 3FE/PT central contact with vapor development.

fuel element at 1273 K contacting a pressure tube at 573 K under 130 N/m uniform lateral FE load. This small value indicates that the spot contact model introduced here is initially appropriate, however in those contact scenarios where contact temperature rises and elastic-plastic deformation occurs, the contact width, will increase.<sup>[21]</sup>

The arc model simulation is presented here is based on the most sensitive contact parameters i.e., contact width and contact conductance. The simulations are performed for either FE/PT or 3FE/PT contact cases where an extra contact region is also considered between FE and PT. Such a contact boundary region is constructed with a very tiny uniform thickness of 2 μm according to the zircaloy roughness of fuel sheath and pressure tube.<sup>[3]</sup> The contact width  $L_c$  and contact conductance  $h$  are varied between 0.1 mm to 4 mm and 0.5 kW/m<sup>2</sup>K to 25 kW/m<sup>2</sup>K, respectively.<sup>[4]</sup>

Figure 7 is obtained for the single FE/PT contact case when two different contact conductances i.e.,  $h_5 = 5 \text{ kW/m}^2\text{K}$  and  $h_{20} = 20 \text{ kW/m}^2\text{K}$  are considered in the contact boundary region. The contact length assumed as  $L_c = 2 \text{ mm}$  and the vapor pockets are constructed with  $\theta = 55^\circ$ . The  $x$  axis is taken as the inner surface of PT or outer surface of FE circumferential arc length according to  $S_3$  in Figure 3. It is clearly shown that when contact conductance decreases ( $h_{20}$  to  $h_5$ ) or contact resistances increases, the temperature difference between FE and PT significantly increases (120 K to 340 K). However, these results also show that the fuel sheath temperature is more sensitive to  $h$  compare to that of obtained for pressure tube inner surface temperature. It is interesting to note that this temperature step change could be increased even more when lower contact conductance is considered at the contact boundary region.

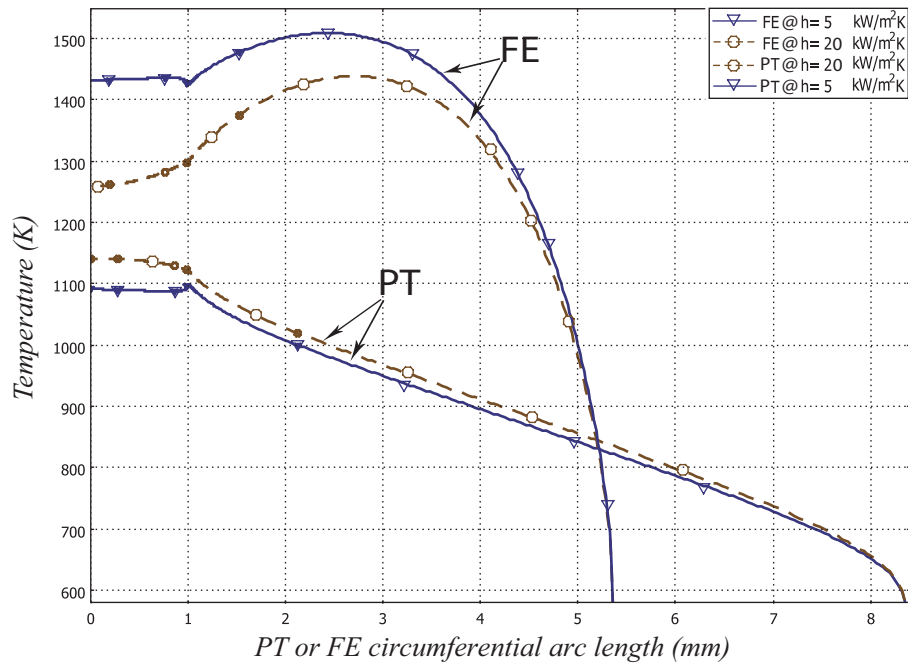


Figure 7. FE/PT temperature profile with different  $h$  at  $L_c = 2 \text{ mm}$  and  $\theta = 55^\circ$ .

Figure 8 shows a temperature profile comparison between single FE/PT contact case with that of obtained for central fuel element at the 3FE/PT contact case. The heat transfer calculations are performed using the contact conductance of  $h_{20} = 20 \text{ kW/m}^2\text{K}$  in both cases a 60 K increase have been achieved in both FE and PT temperature profiles at the contact boundary region. Apparently in this case, the fuel sheath temperature differences are reduced when the circumferential arc length increases while, pressure tube temperature differences are uniformly preserved in whole vapor pocket. This is mainly due to the consideration of the two other fuel elements as compared to the results obtained with a single FE, in which case more heat energy is conducted to the pressure tube.

In the remaining arc model simulations, a sensitivity analysis has been performed in order to obtain the effect of contact width  $L_c$ . In these simulations, once again the vapor pockets are built with  $\theta = 55^\circ$  in the FE/PT contact case along with a contact conductance of  $h_{20} = 20 \text{ kW/m}^2\text{K}$ . It can be seen from Figure 9 that when contact width increases from  $0.1 \text{ mm}$  to  $4 \text{ mm}$  the pressure tube temperature reduces almost by 50 K in the center of contact region. However, the temperature profile in the contact boundary is uniformly decreased in the higher contact width, i.e.,  $1 \text{ mm}$  to  $4 \text{ mm}$ , while it is increased in lower contact width, i.e.,  $0.1 \text{ mm}$  and  $0.5 \text{ mm}$ . This is basically due to the fact that when a very small contact width is considered, the heat conduction through the vapor pocket is high and is dominant when compared to the contact resistance, therefore, the pressure tube temperature in the contact edge is increased mostly by vapor conduction and radiation.

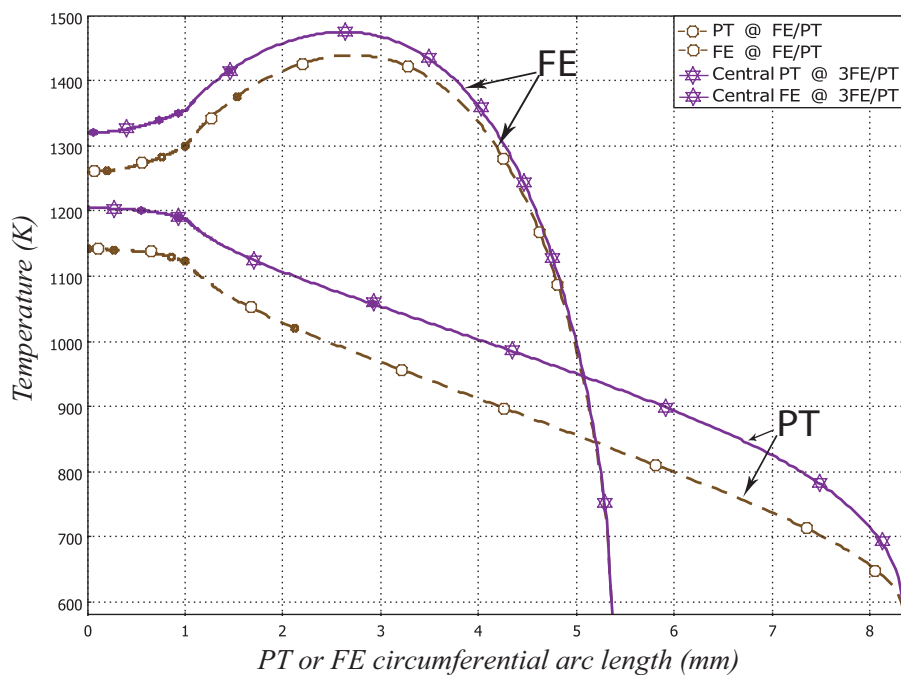


Figure 8. Comparison of FE/PT and 3FE/PT temperature profile at  $L_c = 2 \text{ mm}$  and  $\theta = 55^\circ$ .

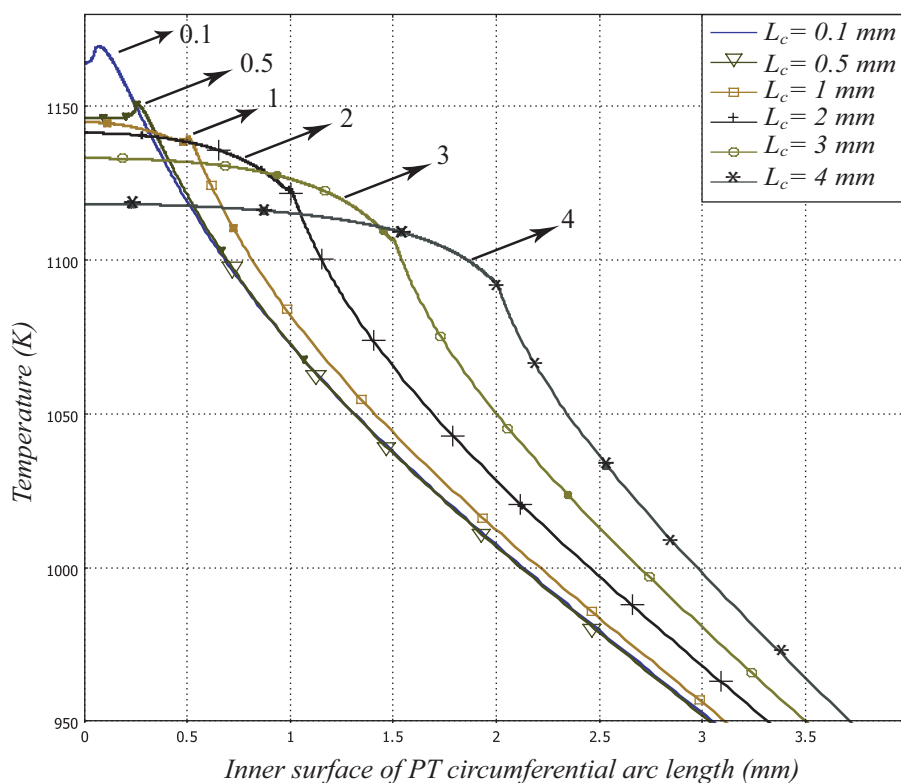


Figure 9. PT temperature profile in FE/PT contact case with  $\theta = 55^\circ$  and different  $L_c$ .

### 3. CONCLUSION

Fuel element to pressure tube contact at full power and highly cooling conditions is considered here in order to investigate potential challenges in fuel channel integrity. We have attempted to simulate several analytical contact models which are the solutions to the steady state heat transfer equations along with appropriate boundary conditions as a primary analysis for the mechanical deformation calculations. The results described here quantify the conditions under which FE/PT or 3FE/PT contact cases could create localized high temperature on the inner surface of a pressure tube. Two different set of simulations have been performed based on contact boundary consideration. The value of parameters considered in these simulations cover a very broad range and in many cases. However, the most sensitive parameters which significantly affecting the contact modelling are i.e., the vapor pocket dimension  $\theta$ , contact conductance  $h$  and contact width  $L_c$ . The results demonstrate the strong sensitivity of maximum pressure tube temperature to the contact conditions and indicate that any local pressure tube deformation will act to reduce the heat transfer to the pressure tube and therefore, will be self-limiting.

### ACKNOWLEDGMENTS

Financial support from the Natural Sciences and Engineering Research Council of Canada (NSERC) and the University Network of Excellence in Nuclear Engineering (UNENE) is gratefully acknowledged.

### REFERENCES

1. R.S.W. Shewfelt, L.W. Lyall, D.P. Godin, "A High-Temperature Creep Model for Zr-2.5 wt% Nb Pressure Tubes", *Journal of Nuclear Materials*, v 125, i 2, p 228-235, (1984).
2. R.S.W. Shewfelt, L.W. Lyall, "A High-Temperature Longitudinal Strain Rate Equation for Zr-2.5 wt% Nb Pressure Tubes", *Journal of Nuclear Materials*, v 132, i 1, p 41-46, (1985).
3. G.R. McGee, M.H. Schankula, M.M. Yovanovich, "Thermal Resistance of Cylinder-Flat Contacts: Theoretical Analysis and Experimental Verification of a Line-Contact Model", *Nuclear Engineering and Design*, v 86, n 3, p 369-81, (1985).
4. D.B. Reeves, P.S. Kundurpi, G.H. Archinoff, A.P. Muzumdar, K.E. Locke, "Analysis of Fuel Element to Pressure Tube Contact Using the MINI-SMARTT Computer Code", *Proc. 7<sup>th</sup> CNS Annual Conf.*, p 156-62, (1986).
5. M.H. Bayoumi, W.C. Muir, P.B. Middleton, "Simulation and Analysis of Bearing Pad to Pressure Tube Contact Heat Transfer under Large Break LOCA Conditions", *Proc. 17<sup>th</sup> CNS Annual Conf.*, Toronto, (1996).
6. V.F. Urbanic, T.R. Heidrick, "High-Temperature Oxidation of Zircaloy-2 and Zircaloy-4 in Steam", *Journal of Nuclear Materials*, 75, p 251-261, (1978).

7. W.C. Muir, M.H. Bayoumi, "Prediction of Pressure Tube Ballooning under Non-Uniform Circumferential Temperature Gradients and High Internal Pressure", *Proc. of the 5<sup>th</sup> Inter. Conf. on Simulation Methods in Nuclear Engineering*, Montreal, (1996).
8. P.M. Mathew, W.C.H. Kupferschmidt, V.G. Snell and M. Bonechi, "CANDU-Specific Severe Core Damage Accident Experiments in Support of Level 2 PSA", *Transactions, SMiRT 16*, Washington DC, (2001).
9. J.C. Luxat, "Mechanistic Modeling of Heat Transfer Processes Governing Pressure Tube to Calandria Tube Contact and Fuel Channel Failure", *Proc. 23<sup>rd</sup> CNS Annual Conf.*, Toronto, (2002).
10. R.W.L. Fong, C.K. Chow, "High-Temperature Transient Creep Properties of CANDU Pressure Tubes", *Proc. 23<sup>rd</sup> CNS Annual Conf.*, Toronto, (2002).
11. Yun Jae Kim, Nam Su Huh, Young Jin Kim, Hyun Kyu Jung, "Estimation of Nonlinear Deflection for Cylinder under Bending and its Application to CANDU Pressure Tube Integrity Assessment", *Nuclear Engineering and Design*, v 223, n 3, p 255-62, (2003).
12. P. Majumdar, D. Mukhopadhyay, S.K. Gupta, H.S. Kushwaha, V. Venkat Raj, "Simulation of Pressure Tube Deformation During High Temperature Transients", *International Journal of Pressure Vessels and Piping*, v 81, n 7, p 575-81, (2004).
13. C. Gerardi, J. Buongiorno, "Pressure-Tube and Calandria-Tube Deformation Following a Single-Channel Blockage Event in ACR-700", *Nuclear Engineering and Design*, v 237, n 9, p 943-954, (2007).
14. F. Talebi, G. Marleau, J. Koclas, "A Model for Coolant Void Reactivity Evaluation in Assemblies of CANDU Cells", *Annals of Nuclear Energy*, v 33, n 11-12, p 975-983, (2006).
15. F. Incropera, D. DeWitt, "Introduction to Heat Transfer", second edition, (1990).
16. K.R. Mayoh, "A Compendium of Material Properties for Zirconium Alloys", COG-96-101, (1997).
17. M. Holmgren, "XSteam for MATLAB, Thermodynamic Properties of Water and Steam", <http://www.mathworks.com>, (2007).
18. S. Glasstone, A. Sesonske, "Nuclear Reactor Engineering", *Krieger Publishing Company*, Malabar, Florida, (1981).
19. O.C. Zienkiewicz, R.L. Taylor, "The Finite Element Method", forth edition, v 2, (1989).
20. COMSOL Heat Transfer Module User's Guide, <http://www.comsol.com>, (2008).
21. M.M. Yovanovich, "Micro and Macro Hardness Measurements, Correlations, and Contact Models", *Collection of Technical Papers - 44<sup>th</sup> AIAA Aerospace Sciences Meeting*, v 16, p 11702-11729, (2006).
22. K.L. Johnson, "Contact Mechanics", *Cambridge University Press*, First Published, (1985).